

# Limits on spin-independent WIMP-nucleon interactions from the two-tower run of the Cryogenic Dark Matter Search

D.S. Akerib,<sup>2</sup> M.J. Attisha,<sup>1</sup> C.N. Bailey,<sup>2</sup> L. Baudis,<sup>11</sup> D.A. Bauer,<sup>3</sup> P.L. Brink,<sup>7</sup> P.P. Brusov,<sup>2</sup> R. Bunker,<sup>9</sup> B. Cabrera,<sup>7</sup> D.O. Caldwell,<sup>9</sup> C.L. Chang,<sup>7</sup> J. Cooley,<sup>7</sup> M.B. Crisler,<sup>3</sup> P. Cushman,<sup>6</sup> M. Daal,<sup>8</sup> R. Dixon,<sup>3</sup> M.R. Dragowsky,<sup>2</sup> D.D. Driscoll,<sup>2</sup> L. Duong,<sup>6</sup> R. Ferril,<sup>9</sup> J. Filippini,<sup>8</sup> R.J. Gaitskell,<sup>1</sup> S.R. Golwala,<sup>12</sup> D.R. Grant,<sup>2</sup> R. Hennings-Yeomans,<sup>2</sup> D. Holmgren,<sup>3</sup> M.E. Huber,<sup>10</sup> S. Kamat,<sup>2</sup> S. Leclercq,<sup>11</sup> A. Lu,<sup>8</sup> R. Mahapatra,<sup>9</sup> V. Mandic,<sup>8</sup> P. Meunier,<sup>8</sup> N. Mirabolfathi,<sup>8</sup> H. Nelson,<sup>9</sup> R. Nelson,<sup>9</sup> R.W. Ogburn,<sup>7</sup> T.A. Perera,<sup>2</sup> M. Pyle,<sup>7</sup> E. Ramberg,<sup>3</sup> W. Rau,<sup>8</sup> A. Reisetter,<sup>6</sup> R.R. Ross,<sup>4,8,\*</sup> B. Sadoulet,<sup>4,8</sup> J. Sander,<sup>9</sup> C. Savage,<sup>9</sup> R.W. Schnee,<sup>2</sup> D.N. Seitz,<sup>8</sup> B. Serfass,<sup>8</sup> K.M. Sundqvist,<sup>8</sup> J-P.F. Thompson,<sup>1</sup> G. Wang,<sup>12,2</sup> S. Yellin,<sup>7,9</sup> J. Yoo,<sup>3</sup> and B.A. Young<sup>5</sup>

(CDMS Collaboration)

<sup>1</sup>*Department of Physics, Brown University, Providence, RI 02912, USA*

<sup>2</sup>*Department of Physics, Case Western Reserve University, Cleveland, OH 44106, USA*

<sup>3</sup>*Fermi National Accelerator Laboratory, Batavia, IL 60510, USA*

<sup>4</sup>*Lawrence Berkeley National Laboratory, Berkeley, CA 94720, USA*

<sup>5</sup>*Department of Physics, Santa Clara University, Santa Clara, CA 95053, USA*

<sup>6</sup>*School of Physics & Astronomy, University of Minnesota, Minneapolis, MN 55455, USA*

<sup>7</sup>*Department of Physics, Stanford University, Stanford, CA 94305, USA*

<sup>8</sup>*Department of Physics, University of California, Berkeley, CA 94720, USA*

<sup>9</sup>*Department of Physics, University of California, Santa Barbara, CA 93106, USA*

<sup>10</sup>*Department of Physics, University of Colorado at Denver and Health Sciences Center, Denver, CO 80217, USA*

<sup>11</sup>*Department of Physics, University of Florida, Gainesville, FL 32611, USA*

<sup>12</sup>*Department of Physics, California Institute of Technology, Pasadena, CA 91125, USA*

We report new results from the Cryogenic Dark Matter Search (CDMS II) at the Soudan Underground Laboratory. Two towers, each consisting of six detectors, were operated for 74.5 live days, giving spectrum-weighted exposures of 34 kg-d for germanium and 12 kg-d for silicon targets after cuts, averaged over recoil energies 10–100 keV for a WIMP mass of 60 GeV/c<sup>2</sup>. A blind analysis was conducted, incorporating improved techniques for rejecting surface events. No WIMP signal exceeding expected backgrounds was observed. When combined with our previous results from Soudan, the 90% C.L. upper limit on the spin-independent WIMP-nucleon cross section is  $1.6 \times 10^{-43}$  cm<sup>2</sup> from Ge, and  $3 \times 10^{-42}$  cm<sup>2</sup> from Si, for a WIMP mass of 60 GeV/c<sup>2</sup>. The combined limit from Ge (Si) is a factor of 2.5 (10) lower than our previous results, and constrains predictions of supersymmetric models.

PACS numbers: 14.80.Ly, 95.35.+d, 95.30.Cq, 95.30.-k, 85.25.Oj, 29.40.Wk

One quarter of the energy density of the universe consists of non-baryonic dark matter [1], which is gravitationally clustered in halos surrounding visible galaxies [2]. The Weakly Interacting Massive Particle (WIMP) [3], a dark matter candidate, arises independently from considerations of Big Bang cosmology and from supersymmetric phenomenology, where the neutralino can be a WIMP [4, 5]. A WIMP has a scattering cross section with an atomic nucleus characteristic of the weak interaction and a mass comparable to that of an atomic nucleus.

The CDMS II experiment [6, 7] is designed to detect recoils of atomic nuclei that have been scattered by incident WIMPs in germanium (Ge) and silicon (Si) crystals. Events with recoil energies of a few tens of keV and rates  $\lesssim 1$  event kg<sup>-1</sup> d<sup>-1</sup> are expected [5, 8]. The CDMS II search is most sensitive to spin-independent (SI) WIMP-nucleon scattering amplitudes [9]. Coherent superposition of SI amplitudes gives Ge better sensitivity than Si, except for small WIMP masses, where kinematics increase the Si sensitivity. In this report we interpret our data with the SI ansatz. Another report describes a

spin-dependent interpretation of our data [10].

The CDMS II apparatus in the Soudan Underground Laboratory has been described elsewhere [6, 7]. At the experiment's core, Z(depth)-sensitive Ionization and Phonon detectors (ZIPs) measure the ionization and athermal phonon signals caused by recoiling particles in Ge and Si crystals [7, 11]. We report new results from the most recent CDMS data run collected between March 25 and August 8, 2004, consisting of 74.5 live days. Six Ge (250 g each) and six Si (100 g each) ZIPs were operated in two vertical stacks ("towers") at a temperature of 50 mK. This report includes the first data from Tower 2, which contains four Si and two Ge ZIPs. Improvements made since the previous run [6, 7] include a reduction of electrical noise and more frequent infrared illumination to clear the crystals of space-trapped charge.

The ZIP detector provides event-by-event discrimination of nuclear recoils from the dominant background of electron recoils. The ratio of ionization energy to phonon energy ("ionization yield") is  $\sim 0.3$  for nuclear recoils, normalized to electron recoils (see yield $\sim 1$  in Fig. 1).

Electron recoils near the detector surface suffer from poor ionization collection and can mimic the ionization yield of nuclear recoils that occur throughout the detector. Each ZIP’s phonon sensors are divided into four quadrants. Timing and signal amplitude comparisons among the quadrants provide discrimination against electron recoils, particularly those near the surface. Also, surface electron recoils often deposit energy in adjacent ZIPs within a tower, causing multiple-detector events. Energy from a WIMP recoil would be contained in one detector.

To avoid bias, we performed blind analyses. Events in and near the signal region were removed from WIMP-search data sets, or “masked” [12]. The cuts that define a signal were determined using calibration data from  $^{133}\text{Ba}$  and  $^{252}\text{Cf}$  sources and from the non-masked WIMP-search data. Seven million electron recoils were collected using a  $^{133}\text{Ba}$  source of gamma rays, exceeding the comparable WIMP-search data by a factor of twenty. Half of the  $^{133}\text{Ba}$  data were used to define analysis cuts and the other half to test cut definitions and estimate expected backgrounds. The detector response to nuclear recoils was characterized with  $10^4$  neutrons from a  $^{252}\text{Cf}$  source, collected in four separate, several-hour periods during the run.

Data from the  $^{133}\text{Ba}$  source were used to monitor detector stability and to characterize detector performance. One Ge detector in Tower 2, ZIP 5 (T2Z5(Ge)), had a spatial region of abnormal ionization response which we excluded from analysis. The Si detector T1Z6, known to be contaminated with  $^{14}\text{C}$ , a beta emitter, was excluded, as were detectors T1Z1(Ge) and T2Z1(Si) due to poor phonon sensor performance. We report results from the remaining 5 Ge and 4 Si ZIPs, chosen before unmasking the WIMP signal region.

Most event selection criteria, based on quantities from the four phonon and two ionization pulses from each detector, are similar to those described in our previous reports [6, 7]. However, we completed five distinct analyses [13] focused on improving existing methods and developing new techniques to reject surface electron recoils. Events with low ionization yield in the  $^{133}\text{Ba}$  calibration data, which are from surface electron recoils, were used to develop rejection criteria. All cuts were frozen prior to unmasking the signal region.

Phonon pulses from surface recoils are more prompt than those from recoils in the detector bulk. Two timing quantities in the quadrant with the largest phonon signal or “local quadrant” are particularly powerful: the time delay of the phonon signal relative to the fast ionization signal, and the phonon pulse risetime [6, 14]. For the first and simplest of the five analysis techniques, the sum of delay and risetime forms a timing parameter, after energy corrections to delay and risetime are applied to achieve an energy-independent distribution. Figure 1 shows the ionization yield versus this timing parameter for a typical Ge detector. The  $^{133}\text{Ba}$  calibration events

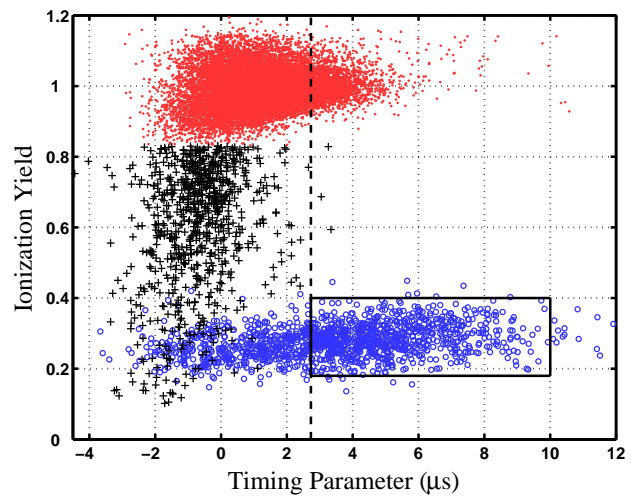


FIG. 1: Ionization yield versus timing parameter (see text) for calibration data in T2Z3(Ge), with recoil energies in the range 10–100 keV. Typical bulk-electron recoils from the  $^{133}\text{Ba}$  source of gamma rays are dots (red), with yield near unity. Low-yield  $^{133}\text{Ba}$  events (+, black), attributed to surface electron recoils, have small values of timing parameter, allowing discrimination from neutron-induced nuclear recoils from  $^{252}\text{Cf}$  (o, blue), which show a wide range of timing parameter values. The vertical dashed line shows the minimum timing parameter allowed for WIMP candidates, and the box shows the approximate signal region, which is in fact weakly energy dependent. (Color online.)

with yields of 0.1 to 0.8, identified as surface electron recoils, show a smaller timing parameter than most nuclear recoils induced by the  $^{252}\text{Cf}$  source.

For data from the Ge detectors, we require that candidates for WIMP-induced nuclear recoil exceed a minimum value for this timing parameter (see Fig. 2 upper-right). Because this “timing parameter” analysis is simple and robust, we agreed before unmasking to report its results. The expected sensitivities computed for the four more advanced analyses described below were all within  $\pm 20\%$  of that computed for this technique.

Two of the four advanced analysis techniques evaluate the goodness of fit,  $\chi^2$ , for surface electron versus bulk nuclear recoil hypotheses. These methods use three variables including their correlations: time delay, risetime, and “partition”. The partition parameter, a measure of energy distribution between the phonon quadrants, is defined as the ratio of phonon energy in the local quadrant to that in the diagonal quadrant. The difference in  $\chi^2$  between surface electron and bulk nuclear recoil hypotheses,  $\Delta\chi^2$ , is used as the principal discrimination parameter in these analyses. One method uses energy-dependent variances and the other energy-independent variances.

For the Si detectors, we decided after unmasking to use the energy-dependent  $\chi^2$  technique, which has the best expected sensitivity to a nuclear recoil signal from low-mass WIMPs for any of our five methods. This analysis

technique is four times as sensitive as the timing parameter analysis for low-mass WIMPs. Before unmasking, we set the minimum requirement on the  $\Delta\chi^2$  for surface electron recoil rejection (see Fig. 2 lower-left). These criteria are used for our WIMP-search results for Si.

The two remaining analysis techniques confirm the robustness of our Ge and Si results. One technique combines delay, risetime and partition in a neural net analysis, and the other technique exploits additional information from the fitted signal pulses to reconstruct recoil position and type. These two and the  $\chi^2$  techniques promise further improvements in sensitivity for the larger exposures planned in our future runs, beyond the improvements already demonstrated in Fig. 2.

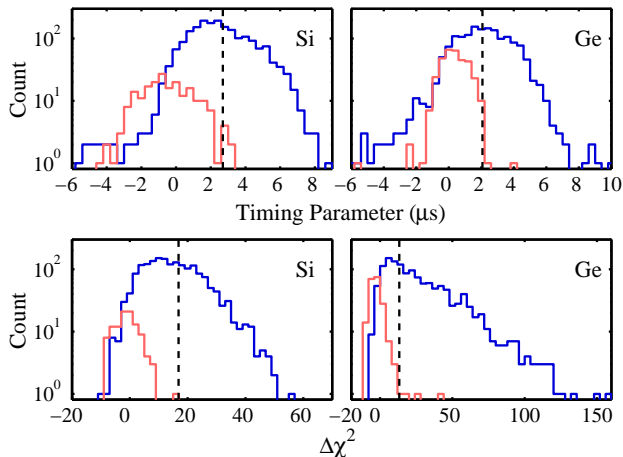


FIG. 2: Variables used to reject surface electron recoils (7–100 keV), for data from T2Z4 (Si/left) and T1Z2 (Ge/right), for the timing parameter (upper) and  $\Delta\chi^2$  (lower). Light (red) lines show distributions of low-yield electron recoils from the  $^{133}\text{Ba}$  source, while dark (blue) lines show distributions of nuclear recoils from the  $^{252}\text{Cf}$  source. Dashed lines indicate the minimum values for acceptable WIMP candidates. A cut on the timing parameter is used for the Ge detectors, while a requirement on  $\Delta\chi^2$  is used for the Si detectors. (Color online.)

Upon unmasking the Ge data, one candidate with 10.5 keV recoil energy was found to pass all cuts in the timing parameter analysis. Unmasking the Si data revealed that no events passed all cuts. Figure 3 shows the unmasked data in ionization yield versus recoil energy; the data before and after application of the cut intended to reject surface electron recoils are shown. All analysis techniques showed consistent results.

After unmasking the Ge data, we realized that the candidate occurred in a detector during an interval of time when that detector suffered inefficient ionization collection. This defect by itself would prevent us from claiming the event was evidence for a WIMP-induced nuclear recoil. The candidate is also consistent with the rate of expected background. Although we do not claim this event as a nuclear recoil from a WIMP, we do include it

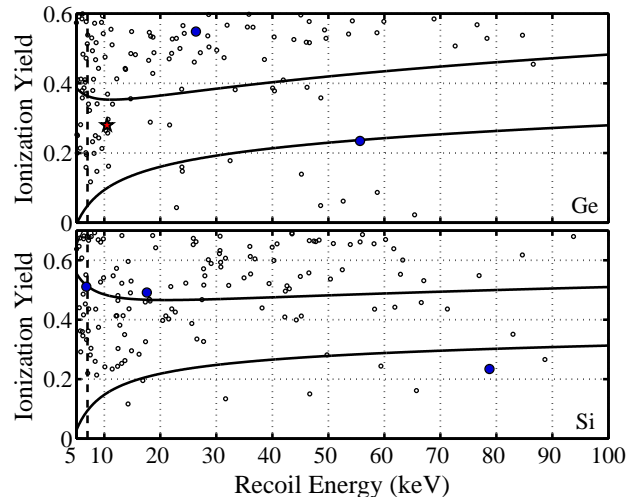


FIG. 3: Ionization yield versus recoil energy for events in all Ge detectors (upper) and all Si detectors (lower) passing initial data selection cuts prior to applying the surface electron recoil rejection cut. The signal region consists of recoil energies exceeding 7 keV, shown with a vertical dashed line, and yields between the curved lines defined with recoils induced by the  $^{252}\text{Cf}$  source while WIMP-search data were still masked. Below 7 keV, separation between nuclear and electron recoils becomes poor. Events passing the surface electron recoil cut are a star (red) inside the signal region and dark filled circles (blue) outside. Bulk-electron recoils with yield near unity are above the vertical scale limits. (Color online.)

in setting limits on the WIMP-nucleon cross section.

The expected surface-event backgrounds are estimated by multiplying two factors. The first factor is the number of events in the signal region before surface-event cuts as obtained upon unmasking. The second factor is the fraction of surface events expected to pass the surface-event cut. This fraction may be estimated with the actual passing fraction of low-yield events similar to the single-detector event background. An estimate using the passing fraction from  $^{133}\text{Ba}$  Ge (Si) data indicates a surface-event background of  $0.13 \pm 0.05$  ( $0.90 \pm 0.4$ ) events. However, we decided before unmasking to base our background estimate on the passing fraction of WIMP-search multiple-detector events in a wide low-yield region. The number of surface events expected to pass the surface-event cuts is  $0.4 \pm 0.2$  (stat)  $\pm 0.2$  (sys) between 10–100 keV in Ge and  $1.2 \pm 0.6$  (stat)  $\pm 0.2$  (sys) between 7–100 keV in Si. Evidence suggests that beta decays of radioactive nuclides distributed across the detectors cause most surface electron recoils in the WIMP-search data. The spatial distribution of these contaminants differs from that of surface electron recoils from the  $^{133}\text{Ba}$  source, which might explain the difference in estimated background levels. From simulation methods reported in [7], the expected background due to cosmogenic neutrons that escape our muon veto is 0.06 events in Ge and 0.05 events in Si.

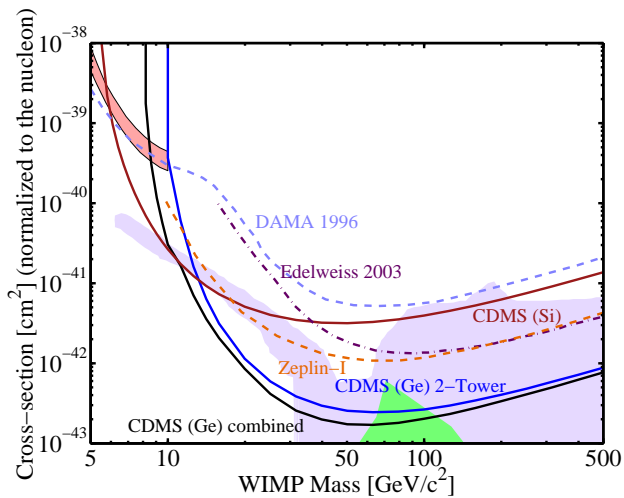


FIG. 4: WIMP-nucleon cross section upper limits (90% C.L.) versus WIMP mass. The upper CDMS Ge curve also uses data from the current run, while the lower Ge curve includes data from the previous run [6]. Supersymmetric models allow the largest shaded (light-blue) region [15], and the smaller shaded (green) region [17]. The shaded region in the upper left (see text) is from DAMA [18], and experimental limits are from DAMA [16], EDELWEISS [19], and ZEPLIN [20]. (Color online.)

Figure 4 shows the upper limits on WIMP-nucleon cross sections calculated from the Ge and Si analyses reported here using standard assumptions for the galactic halo [8]. For the upper Ge limit, data between 10–100 keV from this run are used. Also shown is the combined limit obtained from this report and our earlier work [6, 7]. For the combined Ge limit, we have included data in the 7–10 keV interval of recoil energy from the run reported here [21]. The combined result for Ge limits the WIMP-nucleon cross-section to  $< 1.6 \times 10^{-43} \text{ cm}^2$  at the 90% C.L. at a WIMP mass of  $60 \text{ GeV}/c^2$ , a factor of 2.5 below our previously published limits. This new Ge limit constrains some minimal supersymmetric (MSSM) parameter space [15] and for the first time excludes some parameter space relevant to constrained models (CMSSM) [17].

The Si limit in Fig. 4 is based on standard halo assumptions using Si data from 7–100 keV in this run. The Si result limits the WIMP-nucleon cross-section to  $< 3 \times 10^{-42} \text{ cm}^2$  at the 90% C.L. at a WIMP mass of  $60 \text{ GeV}/c^2$ . This Si result excludes new parameter space for low-mass WIMPs, including a region compatible with interpretation of the DAMA signal (2–6 and 6–14 keV bins) as scattering on Na [18].

This work is supported by the National Science Foundation under Grant Nos. AST-9978911 and PHY-9722414, by the Department of Energy under contracts DE-AC03-76SF00098, DE-FG03-90ER40569, DE-FG03-91ER40618, DE-FG02-94ER40823, and by Fermilab, operated by the Universities Research Association, Inc., under Contract No. DE-AC02-76CH03000 with the Depart-

ment of Energy. The ZIP detectors were fabricated in the Stanford Nanofabrication Facility operated under NSF.

\* Deceased

- [1] D. N. Spergel *et al.*, (WMAP Collab.), *Astrophys. J. Suppl.* **148**, 175 (2003); M. Tegmark *et al.*, (SDSS Collab.), *Phys. Rev. D* **69**, 103501 (2004).
- [2] P. Salucci and A. Borriello, *Lect. Notes Phys.* **616**, 66 (2003); T. Broadhurst *et al.*, *Astrophys. J.* **621**, 53 (2005).
- [3] G. Steigman and M.S. Turner, *Nucl. Phys.* **B253**, 375 (1985).
- [4] B.W. Lee and S. Weinberg, *Phys. Rev. Lett.* **39**, 165 (1977); S. Weinberg, *Phys. Rev. Lett.* **48**, 1303 (1982).
- [5] G. Jungman, M. Kamionkowski, and K. Griest, *Phys. Rep.* **267**, 195 (1996); G. Bertone, D. Hooper, and J. Silk, *Phys. Rep.* **405**, 279 (2005).
- [6] D.S. Akerib *et al.*, (CDMS Collab.) *Phys. Rev. Lett.* **93**, 211301 (2004).
- [7] D.S. Akerib *et al.*, (CDMS Collab.), accepted for PRD. arXiv:astro-ph/0507190 (2005).
- [8] J.D. Lewin and P.F. Smith, *Astropart. Phys.* **6**, 87 (1996).
- [9] A Majorana neutralino undergoes a scalar interaction of roughly equal strength for neutrons and protons, see K. Griest *Phys. Rev. D* **38**, 2357 (1988). The SI scattering amplitude is generally sensitive to scalar, vector, and tensor interactions of a spin-1/2 WIMP, see A. Kurylov and M. Kamionkowski, *Phys. Rev. D* **68**, 103509 (2003).
- [10] D.S. Akerib *et al.*, (CDMS Collab.), submitted to *Phys. Rev. Lett.*
- [11] K.D. Irwin *et al.*, *Rev. Sci. Instr.* **66**, 5322 (1995); T. Saab *et al.*, *AIP Proc.* **605**, 497 (2002).
- [12] Although software safeguards to enforce the blinding scheme did not work as intended, the blinding policy itself remained in effect, and we exercised care not to obtain any information from inside the WIMP-search signal region. We believe the cuts were developed fully blind.
- [13] CDMS collaboration, in preparation for *Phys. Rev. D*; theses and notes at <http://cdms.berkeley.edu/Dissertations>.
- [14] R.M. Clarke *et al.*, *Appl. Phys. Lett.* **76**, 2958 (2000).
- [15] A. Bottino *et al.*, *Phys. Rev. D* **69**, 037302 (2004).
- [16] R. Bernabei *et al.*, *Phys. Lett. B* **389**, 757 (1996).
- [17] J. Ellis, *et al.*, *Phys. Rev. D* **71**, 095007 (2005).
- [18] We show the 90% allowed region from Fig. 2a of P. Gondolo and G. Gelmini, *Phys. Rev. D* **71**, 123520 (2005).
- [19] V. Sanglard *et al.*, (EDELWEISS Collab.), *Phys. Rev. D* **71**, 122002 (2005).
- [20] G.J. Alner *et al.*, (UK Dark Matter Collab.), *Astropart. Phys.* **23**, 444 (2005).
- [21] Cuts for 7–10 keV interval of recoil energy were frozen before data were unmasked. The decision to report these data was made after the unmasking. Inclusion of this interval increases the expected background by  $0.1 \pm 0.02(\text{stat})$  events, and lowers the limit on WIMP-nucleon cross section only for WIMP masses in the 8–11  $\text{GeV}/c^2$  interval. No candidate events were found in the 7–10 keV interval of recoil energy.